

# Backtracking Search Algorithm for Non-Aligned Thrust Optimization for Satellite Formation\*

Soyinka Olukunle Kolawole, Haibin Duan, *Senior Member, IEEE*

**Abstract—** This paper considers the effect of an optimized non-aligned thrust on formation keeping of multiple satellites. In particular, comparison is made between the performances of the regular thrust configuration and the non-aligned case. The relative dynamics of motion for the formation is based on the Gauss variational equations. The optimization of the non-aligned thrust inclination angles was done via chaotic backtracking search algorithm. Finally a state feedback control law for formation keeping was used with constraints for actuator saturation also implemented. Simulation results indicate the effectiveness of non-aligned thrust in maintaining  $J_2$  invariant relative orbit at steady state.

## I. INTRODUCTION

Quite recently, considerable attention has been paid to the subject of satellite formation flying control because of the advantages of multiple satellite constellations over a single monolithic satellite such as the ability to reconfigure a swarm of satellites in the event of a single point failure. Satellite formation control is defined as “the tracking or maintenance of a desired relative separation, orientation or position between or among satellites” [1]. Maintaining a formation in a particular configuration either throughout the entire orbit or at certain times during the orbit is critical to surveillance missions, remote sensing and communications to mention a few, these underscore the importance of formation keeping methods. The literature on the subject shows various approaches to solving the two main concerns for satellite formation control, namely, formation maintenance and reconfiguration. In Refs. [2,3,4,5] research focused on formation keeping of multiple satellites using methods such as model predictive control and robust control for formation keeping and attitude control. Formation keeping spans the orbit life of a satellite, hence the need for optimal solutions to the formation keeping problem; Refs. [6,7,8,9] sought to design formations that minimized fuel consumption. Ref.[10] used a distributed control algorithm for multiple spacecraft in close proximity operations, the algorithm was developed using a combination of artificial potential function and linear quadratic regulator.

\*This work was partially supported by Aeronautical Foundation of China under grant #20135851042

Soyinka Olukunle Kolawole is with the School of Automation Science and Electrical Engineering Beihang University (BUAA), China (e-mail: kunlesoyinka@yahoo.com)

Haibin Duan is with the Science and Technology on Aircraft Control Laboratory, School of Automation Science and Electrical Engineering, Beihang University (BUAA), China (e-mail: hbduan@buaa.edu.cn).

The use of heuristic methods is beginning to gain prevalence in control engineering as is evidenced in Ref.[11], these methods have been studied and applied to satellite formation reconfiguration problem in Refs [12, 13, 14]. The majority of these spacecraft formation keeping methods use thrusters as control actuator and implicitly assume that the thrusters will produce pure thrust vectors along the principal directions of the body axes. This paper conducts research into the effect of non-aligned thrust vectors (NATV) on formation keeping and seeks to determine optimal thrust inclination angles that will yet minimize a fuel consumption dependent cost function. The studies in this paper follow the trend of utilizing heuristic methods in formation flying control by implementing the chaotic backtrack search algorithm (CBSA) in optimizing the non-aligned thrust vectors. An advantage of implementing a chaotic form of the algorithm over the regular algorithm lies in the spread-spectrum, non-periodic and ergodic properties that chaotic sequences possess over the random sequence generator [15]. The remainder of the paper is organized as follows. Section II describes the dynamic equations that model our pair of satellite in formation, the aligned and non-aligned thruster configuration and underlying control law. Section III presents a detailed description of the chaotic backtrack search algorithm (CBSA). Section IV presents simulation studies while conclusion is presented in section V.

## II. SATELLITE FORMATION MODEL DYNAMICS

The relative motion of satellites in a formation can be described using the Gauss variational equations (GVE) in Ref. [16]. The GVE provides a means of calculating analytically the differential changes that occur in the orbital element set provided knowledge of the perturbing forces are available. Our dynamic model makes use of the GVE including  $J_2$  perturbation. We state the GVE here for convenience

$$\left\{ \begin{aligned} \frac{da}{dt} &= \frac{2a^2}{h} \left( e \sin f u_r + \frac{p}{r} u_\theta \right) \\ \frac{de}{dt} &= \frac{1}{h} (p \sin f u_r + ((p+r) \cos f + re) u_\theta) \\ \frac{di}{dt} &= \frac{r \cos \theta}{h} u_h \\ \frac{d\Omega}{dt} &= \frac{r \sin \theta}{h \sin i} u_h - \frac{3}{2} J_2 \left( \frac{R}{p} \right)^2 \sqrt{1-e^2} \cos i \\ &\quad + \frac{3}{4} J_2 \left( \frac{R}{p} \right)^2 \sqrt{1-e^2} (5 \cos^2 i - 1) \\ \frac{d\omega}{dt} &= -\frac{p \cos f u_r}{he} + \frac{(p+r) \sin f u_\theta}{he} - \frac{r \sin \theta \cos i u_h}{h \sin i} \\ \frac{dM}{dt} &= \sqrt{\frac{\mu}{a^3}} + ((p \cos f - 2re) u_r - (p+r) \sin f u_\theta) \times \frac{\sqrt{1-e^2}}{he} \\ &\quad + \frac{3}{4} J_2 \left( \frac{R}{p} \right)^2 \sqrt{1-e^2} \sqrt{\frac{\mu}{a^3}} (3 \cos^2 i - 1) \end{aligned} \right. \quad (1)$$

where  $a$  is semi-major axis,  $e$  is eccentricity,  $f$  is true anomaly,  $i$  is the inclination,  $\Omega$  is right ascension of ascending node,  $\omega$  is argument of periapsis,  $M$  is mean anomaly,  $p$  is semi latus rectum,  $\theta$  is the true latitude,  $h$  denotes angular momentum,  $\mu$  is earth gravitation parameter,  $r$  is scalar orbital radius,  $R$  is the equatorial radius of earth,  $J_2$  is perturbation constant,  $U_r$ ,  $U_\theta$  and  $U_h$  represents thrust in the satellites LVLH (local vertical local horizontal) frame.

If we define a satellite's state vector using the mean orbital elements as  $X = [a \ e \ i \ \omega \ \Omega \ M]^T$ , then the equations of motion including  $J_2$  perturbation can be written in matrix form as in Ref. [17].

$$\dot{X} = \begin{bmatrix} 0 \\ 0 \\ 0 \\ -\frac{3}{2} J_2 \left( \frac{R}{p} \right)^2 \sqrt{1-e^2} \cos i \\ \frac{3}{4} J_2 \left( \frac{R}{p} \right)^2 \sqrt{1-e^2} (5 \cos^2 i - 1) \\ \sqrt{\frac{\mu}{a^3}} \left( 1 + \frac{3}{4} J_2 \left( \frac{R}{p} \right)^2 \sqrt{1-e^2} (3 \cos^2 i - 1) \right) \end{bmatrix} + \begin{bmatrix} \frac{2a^2 e \sin f}{h} & \frac{2a^2 p}{h} & 0 \\ \frac{p \sin f}{h} & \frac{(p+r) \cos f + re}{h} & 0 \\ 0 & 0 & \frac{r \cos \theta}{h} \\ 0 & 0 & \frac{r \sin \theta}{h \sin i} \\ \frac{-p \cos f}{ha} & \frac{(p+r) \sin f}{ha} & \frac{-r \sin \theta \cos i}{h \sin i} \\ \frac{\sqrt{1-e^2} (p \cos f - 2re)}{ha} & \frac{-\sqrt{1-e^2} (p+r) \sin f}{ha} & 0 \end{bmatrix} \begin{bmatrix} U_x \\ U_y \\ U_z \end{bmatrix} \quad (2)$$

In the above equation, we have replaced  $U_r$ ,  $U_\theta$  and  $U_h$  with  $U_x$ ,  $U_y$  and  $U_z$  respectively assuming LVLH frame aligns with the deputy satellite's nominal axis. The GVE equations are then applied to the mean orbit element differences as follows. In a leader-follower configuration the formation is expected to maintain a fixed bounded relative motion but in the presence of perturbation this does not hold true; the position of the follower can be described using the mean orbit element as

$$e_{fd} = e_{lead} + \Delta_{ef} \quad (3)$$

where  $e_{fd}$  represent the desired mean orbital elements of the follower satellite;  $e_{lead}$  is the mean orbital element of the leader satellite and  $\Delta_{ef}$  is the desired relative orbital element difference of the follower denoted as

$$\Delta_{ef} = [\delta a, \delta e, \delta i, \delta \omega, \delta \Omega, \delta M] \quad (4)$$

However due to perturbations the desired geometry is never fixed so we express this error as

$$\delta_f = e_{fpert} - e_{fd} \quad (5)$$

where  $e_{fpert}$  gives the follower satellite's mean orbital elements due to perturbation,  $e_{fd}$  is the desired, mean orbital elements of the follower and  $\delta_f$  is the error. By Taylor's series expansion the error rate can be expressed as

$$\dot{\delta}_f = \dot{e}_{fpert} - \dot{e}_{fd} \quad (6)$$

This gives rise to the state space form

$$\dot{\delta}_f = A(e_{fd}) \delta_f + B(e_{fd}) U \quad (7)$$

with a discrete approximation of the state space written as

$$\delta_f(k+1) = A(e_{fd}) \delta_f(k) + B(e_{fd}) U(k) \quad (8)$$

We apply the approximate control law  $U(k)$  developed in Ref. [5]

$$U = \begin{bmatrix} u_x \\ u_y \\ u_z \end{bmatrix} = - \left( [B]^T [B] \right)^{-1} [B]^T \left( [A(e_{fd})] + [K] \right) \delta_f \quad (9)$$

where  $K$  is the feedback gain matrix and  $A(e_{fd})$  is a matrix containing all zeros except the  $3 \times 3$  elements of the lower left corner thus we obtain

$$A(e_{fd}) = \begin{bmatrix} 0_{3 \times 3} & 0_{3 \times 3} \\ \Phi_{3 \times 3} & 0_{3 \times 3} \end{bmatrix} \quad (10)$$

And the matrix elements can be written as

$$\left\{ \begin{aligned} \varphi_{11} &= \frac{21 J_2 (R - e^2)^2 \sqrt{\mu} \cos i}{4 a^4 \sqrt{a}} \\ \varphi_{12} &= 6 J_2 \cos i \sqrt{\frac{\mu}{a^7}} (R - e^3) \\ \varphi_{13} &= \frac{3 J_2 (R - e^2)^2 \sqrt{\frac{\mu}{a^7}} \sin i}{2} \\ \varphi_{21} &= \frac{-21 J_2 (R - e^2)^2 \sqrt{\mu} (5 \cos^2 i - 1)}{8 a^4 \sqrt{a}} \\ \varphi_{22} &= 3 J_2 \cos i \sin i \sqrt{\frac{\mu}{a^7}} (e^3 - R) (5 \cos^2 i - 1) \\ \varphi_{23} &= \frac{15 J_2 (R - e^2)^2 \sqrt{\frac{\mu}{a^7}} \sin i \cos i}{2} \\ \varphi_{31} &= \frac{27 J_2 (R)^2 (3 \cos^2 i - \frac{1}{3})}{(2 a \sqrt{a} (1 - e^2)^{3/2} + 1)} - \frac{9 J_2 (R)^2 (3 \cos^2 i - \frac{1}{3})}{2 a^3 (1 - e^2)^{3/2}} \\ \varphi_{32} &= \frac{9 J_2 (R)^2 \sqrt{\frac{\mu}{a^3}} (3 \cos^2 i - 1)}{4 a^2 (1 - e^2)^{\frac{5}{2}}} \\ \varphi_{33} &= \frac{-18 J_2 (R)^2 \cos i \sin i}{(4 a^2 (1 - e^2)^{3/2} + 1) \sqrt{\frac{\mu}{a^3}}} \end{aligned} \right. \quad (11)$$

Our purpose is to investigate the effectiveness of using non aligned thrust as is present in a gimballed thruster to drive the state error to nullity. To do this we pose an optimization problem such that optimal values of the

inclination angles are obtained while minimizing fuel consumption. To obtain the relative orbit motion we employ the set of equations in Ref. [16] that maps the orbital element differences to the Cartesian coordinates; the equations are stated here

$$\begin{cases} x(f) = (1 - e \cos f) \delta a + \frac{a e \sin f}{\Upsilon} \delta M - a \cos f \delta e \\ y(f) = \frac{a}{\Upsilon} (1 - e \cos f) \delta M + a (1 - e \cos f) \delta \omega \\ \quad + a \sin f (2 - e \cos f) \delta e + a (1 - e \cos f) \cos i \delta \Omega \\ z(f) = a (1 - e \cos f) (\sin \theta \delta i - \cos \theta \sin i \delta \Omega) \end{cases} \quad (12)$$

where

$$\Upsilon = (1 - e^2)^{1/2} \quad (13)$$

and  $\delta a, \delta e, \delta i, \delta \Omega, \delta \omega, \delta M$  are the differences in semi major axis, eccentricity, inclination, right ascension of ascending node (RAAN), argument of periapsis and mean anomaly respectively;  $f$  is the true anomaly while  $a, e$  and  $i$  retain their earlier definitions. In this study we take our regular thruster configuration as a simplistic arrangement called aligned thrust vector (ATV) configuration shown in Fig.1. The Z-axis is positive in a direction moving into the paper. The minimum fuel problem is formulated as one that finds the infimum of the sum of applied control forces.

$$P_1 = \sum_{t=t_0}^{t=t_f} (U_x^2 + U_y^2 + U_z^2)^{1/2} \quad (14)$$

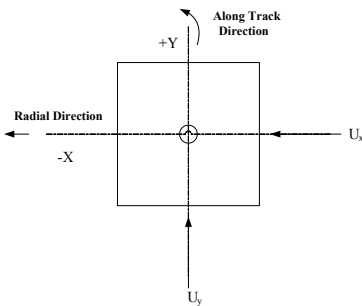


Figure 1. Nominal configuration (X - Y plane)

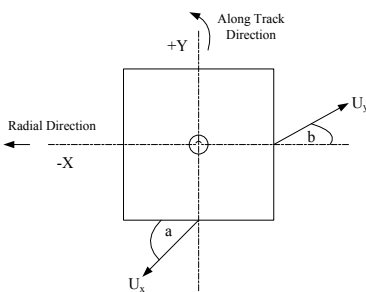


Figure 2. Non-aligned configuration (X-Y plane)

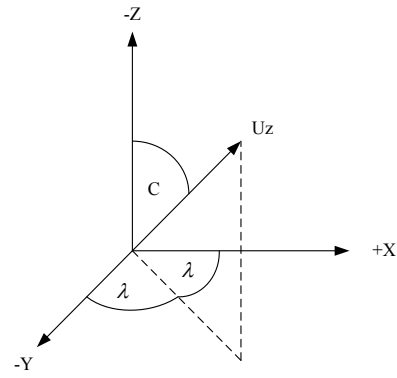


Figure 3. Non-aligned configuration (XYZ)

If the thrust vector  $[U_x \ U_y \ U_z]^T$  is not aligned along the nominal body axes  $(X_b, Y_b, Z_b)$  of the deputy satellite, as in Fig. 2 and Fig. 3, parasitic moments will be induced about the center of mass of the satellite. Since our consideration is the maintenance of the relative distance we assume the existence of attitude stabilization mechanism to maintain gyroscopic rigidity of the deputy satellite. The thrust vector then becomes

$$[-U_x (\cos a + \sin a) \ U_y (\cos b + \sin b) \ U_z \cos c]^T .$$

The complexity of the formulation is relaxed by assuming that the angle between negative Y-axis and projection of  $U_z$  onto the X-Y plane is same as that with the X-axis (see Fig. 3), then the problem is modified thus

#### Problem Statement

$$\min P_2 = \sum (U_x^2 + U_y^2 + U_x \sin(2a) + U_y \sin(2b) + U_z^2 \cos^2 c)^{1/2} \quad (15)$$

s.t

- i.  $\dot{X} = AX + BU$
- ii.  $-U_{max} \leq U \leq U_{max}$
- iii.  $\left[ \pi + \frac{\pi}{6} \right] \leq a \leq \left[ \pi + \frac{\pi}{3} \right]$
- iv.  $\frac{\pi}{18} \leq b \leq \frac{\pi}{3}$
- v.  $\frac{\pi}{18} \leq c \leq \frac{\pi}{3}$

where the parameters  $a, b, c$  represent inclination angles. This study has applied the optimal control thrust to a leader and one follower satellite but a distributed control scheme is implementable for multiple follower satellites and one leader satellite as shown in Fig 4. Where each follower is controlled to maintain its desired position relative to the leader satellite.

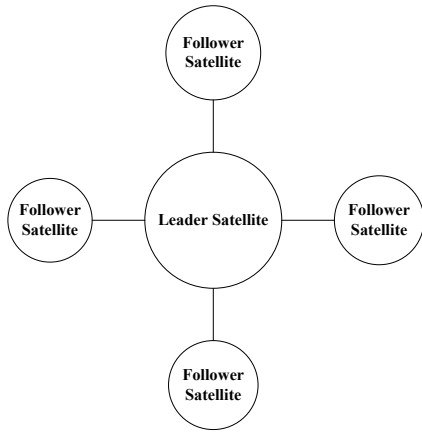


Figure 4. Leader satellite and multiple follower satellite

Each follower satellite is assumed to have sensors to estimate its position relative to the leader in a frame coincident with the position of the leader satellite. For  $N$  follower satellites in a formation the constraints of optimization can be generalized as

- i.  $\dot{X}^i = AX^i + BU^i \quad i \in \{1, 2, 3, \dots, N\}$
- ii.  $U^i \in (-U_{max}, U_{max}] \quad i \in \{1, 2, 3, \dots, N\}$

and also iii – iv above.

### III. CHAOTIC BACKTRACK SEARCH ALGORITHM (CBSA)

To minimize  $P_2$  in Eq. (15) we rely on numerical optimization technique. Each individual in the algorithm is associated with our unknown variables a, b and c that represents inclination angles for the thrust vectors. In the following sub-sections we describe the algorithm. The backtracking search algorithm (BSA) in Ref. [18] is a new evolutionary algorithm for solving real-valued numerical optimization problem. The CBSA is a variant of the basic BSA where a chaotic map (this is denoted  $Cr$  in the initialization phase) is used in place of the random generator at the initialization phase; this improves the ergodicity of the system. The detailed algorithm is presented below.

#### A. Initialization

In the initialization phase the CBSA generates an initial and old population based on the expression

$$pop_{ij} = Cr.(Upper\ limit - lower\ limit) + lower\ limit \quad (16)$$

$$oldpop_{ij} = Cr.(Upper\ limit - lower\ limit) + lower\ limit \quad (17)$$

$i \in 1, 2, 3, \dots, N$  and  $j \in 1, 2, 3, \dots, D$ .  $N$  and  $D$  being population size and dimension respectively while  $P_i$  is the target individual. At the start of each iteration CBSA can redefine the old population using the if-then conditional that

$$if\ \alpha < \delta\ then\ OldP := P \quad (18)$$

where  $\alpha$  and  $\delta$  are random numbers, individuals in the old population are then shuffled by permuting.

#### B. Mutation

The mutation process generates the initial form of the trial population called Mutant using the expression

$$Mutant = P + F(oldP - P) \quad (19)$$

where  $F$  is the scale factor and it controls the search direction matrix ( $oldP - P$ ).  $F$  can be evaluated using

$$F = 3 \cdot randn \quad (20)$$

#### C. Crossover

The final form of the trial population ( $T$ ) is generated in the crossover process. The initial value of  $T$  is set to the result of the mutation process above.

$$T = Mutant \quad (21)$$

The crossover process has two distinct steps; the first involves initializing a binary integer-valued matrix of size ( $N \cdot D$ ) denoted

$$map_{n,m} \quad n \in \{1, 2, 3, \dots, N\} \quad m \in \{1, 2, 3, \dots, D\} \quad (22)$$

and the second step involves the strategy that defines the number of individuals that mutate in a trial; and this is done in two ways. The first way entails specifying a mix rate parameter to define the number of elements of individuals that will mutate in a trial and the second way allows only one individual to mutate at each trial.

#### D. Selection II

In this phase, a greedy selection is used to update all trial populations ( $T_i$ ) with better fitness values with respect to ( $P_i$ ). If the best individual  $P(P_{best})$  has better fitness values than the global minimum obtained by CBSA so far then  $P_{best}$  is taken as the global minimizer and the fitness of  $P_{best}$  is taken as the global minimum.

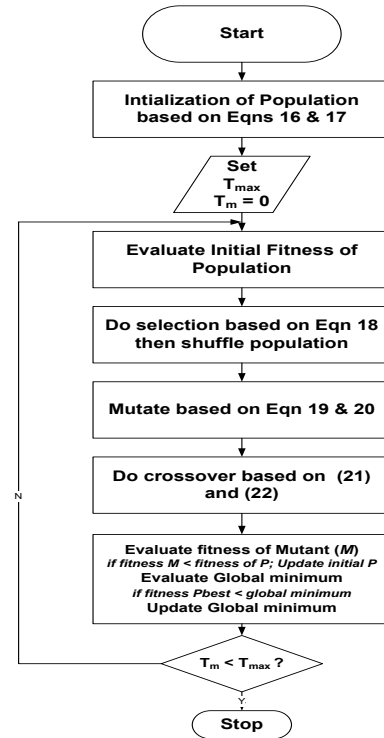


Figure 5. Flow chart for our proposed CBSA

The sequence of operation for the satellite formation keeping is illustrated in Fig. 6.

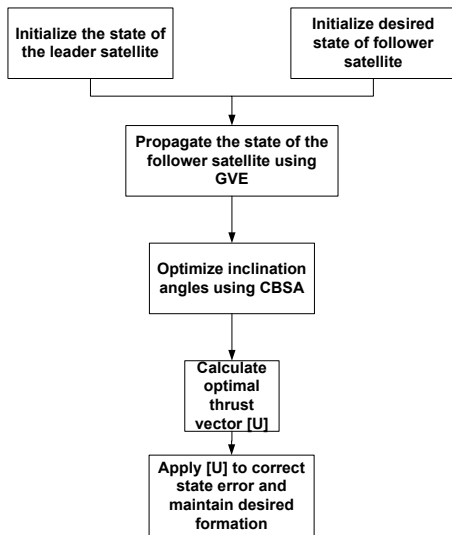


Figure 6. Sequence of operation for formation keeping

#### IV. SIMULATION STUDIES AND RESULTS

In this section, we present the results of our studies on formation keeping control under the influence of NATV compared with ATV. Our formation consists of a deputy satellite and a leader. The following parameters are assumed; Initial population = 40; dimension = 3; maximum iteration = 1000; boundary limits are set using constraints (iii), (iv) and (v) earlier stated. The following states are assumed for the leader satellite, deputy satellite and the desired formation:

Leader Satellite:

[6587.63 0.030005 10.0 0.0 49.895 28.177]

Deputy Satellite:

[6586.278 0.0301005 10.001035 0.005 49.905 28.167]

Desired Relative State:

[-0.351765 0.0001 0.001035 0.005 0.01 -0.01]

$$K = \begin{bmatrix} 0.0684918768929111 & 0.0164512223009252 \\ 0.0396435028405985 & 0.0101940123462108 \\ 0.0985013578957873 & 0.0615226543981972 \end{bmatrix}$$

$$U_{\max} = [0.01 \ 0.01 \ 0.01]^T$$

In the first simulation we obtain optimal thrust inclination angles for the cost function in (16) by comparing the result of PSO [19] and CBSA (see Fig. 6 and Table I). In the second simulation we verify experimentally the better of the two thruster configurations by applying the results of our earlier simulation to our control law.

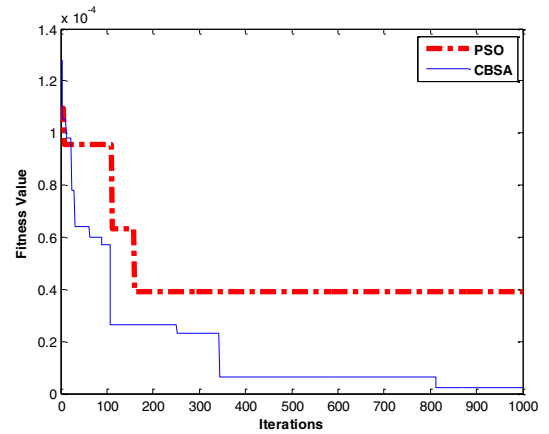


Figure 7. Fitness curves comparison of CBSA and PSO

Table I Optimal Inclination Angles

EA	Optimal Values			
	<i>a</i> (radian)	<i>b</i> (radian)	<i>c</i> (radian)	Fitness value
PSO	3.93901171	0.811246808	0.779277495	0.0000
	1669864	080921	430632	4213
CBSA	4.01260297	0.776898428	0.753552169	0.0000
	5593089	109911	207761	1388

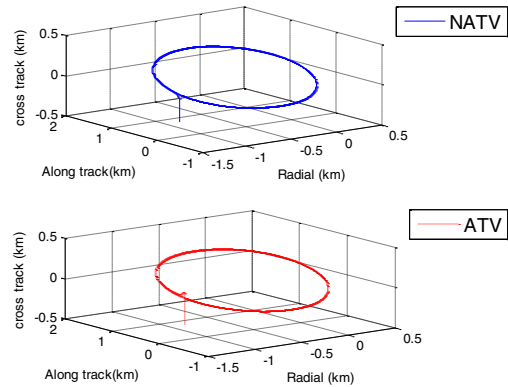


Figure 8. Relative motion ATV/NATV after two orbits

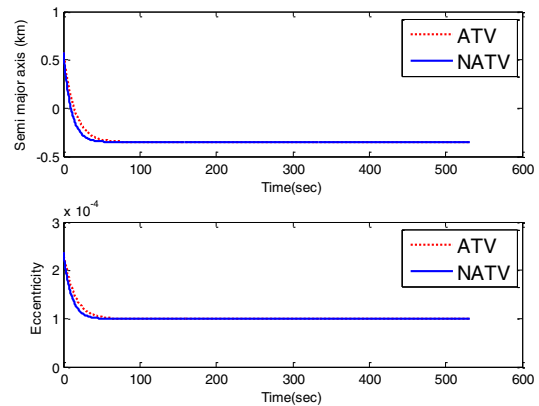


Figure 9. Semi-major axis and Eccentricity Error ATV/NATV

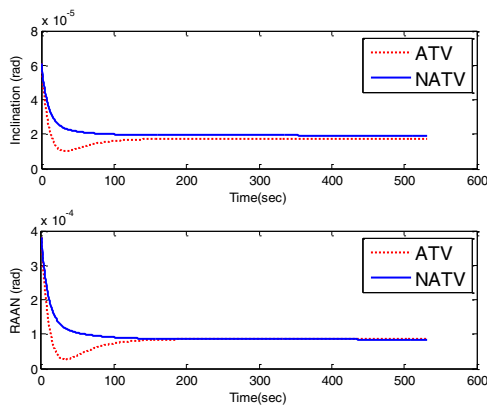


Figure 10. Inclination and RAAN error ATV/ NATV

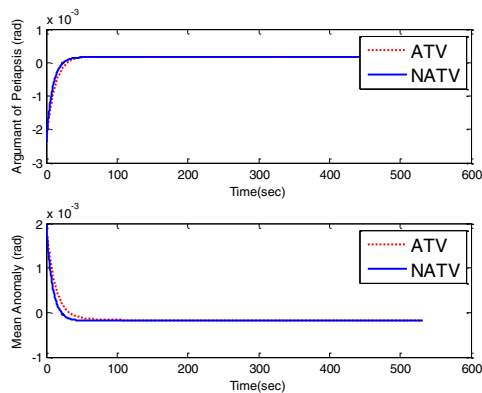


Figure 10. Argument of perigee and mean anomaly error ATV/NATV

In both cases, the mean orbital elements of the deputy satellite asymptotically converge towards the desired relative state with a slightly better performance for the NATV in tracking the desired relative states of the deputy satellites. Specifically, the initial overshoot in ATV is higher when compared to NATV (see Fig.7).

## V. CONCLUSION

This paper investigated the effectiveness of non-aligned thrusts on satellite formation keeping control by finding optimal inclination angles that minimize amount of fuel consumed. The results of our simulation demonstrate that though both methods will eventually cancel out the disturbance and the formation is maintained at steady states. Practical application for non-aligned thrust is found in gimbaled thrusters used in launch rockets; one motivation for this study is to look at the feasibility of this type of thrusters for formation maintenance. The present scope of this study has limited the leader satellite to a near circular orbit and the controller feedback gain implemented was a fixed scalar quantity; taking advantage of orbital motion suggests that the feedback gain could be non-constant. The authors intend to consider these in their future studies and also apply a novel Pigeon-inspired Optimization (PIO) [20] for solving satellite formation reconfiguration problems.

## REFERENCES

1. M. Paluzek, B. Pradeep, P. Griesemer, J. Mueller, S. Thomas, *Satellite Attitude and Orbit Control*, Second Edition, Princeton satellite systems, NJ, pp. 128, 1996.

2. V. Manikonda, P. Arambel, M. Gopinathan, R. Mehra, F.Y Hadaegh, "A model predictive-based approach for spacecraft formation keeping and attitude control", in *Proc of the American Control Conference*, San Diego USA, pp. 4258-4262, June 1999.
3. M. Milam, N. Petit, R. Murray, "Constrained trajectory generation for micro-satellite formation flying", AIAA Guidance Navigation and Control Conference and Exhibit, Canada, A01-37015, August 2001.
4. T. Duc Le, K. Furusawa, T. Hayakawa, "Orbital formation control of multiple satellites", 2010 American Control Conference, Baltimore USA, pp. 3636-3641, 2010.
5. X.C. Yue, Y. Yang, Z.S. Duan, Z.Y. Geng. "Parameter-dependent lyapunov function method applied to satellite formation keeping control", in *Proc of the 27th Chinese Control Conference*, Yunnan China, pp. 761-765, July 2008.
6. B. Wu, E. KeePoh, G. Xu, "Satellite formation keeping via real-time optimal control and iterative learning control", 2009 *IEEE Aerospace Conference*, paper #1218, Version 2, pp 1-8.
7. H. He, Z. Jun, Y.Y. Li., "Fuel-balanced satellite formation keeping research", IEEE International Conference on Intelligent Computing and Intelligent Systems, China, pp 16-20, Oct 2010.
8. K. Yamada, M. Kimura, I. Jikuya, "Fuel-optimal eccentricities for precise formation keeping of keplerian orbits", *Acta Astronautica*, Vol.68, pp. 1811-1819, 2011.
9. M. Ross, K. Jeffery, F. Fahroo, "Designing optimal spacecraft formations", AIAA/AAS Astrodynamics Specialist conference and exhibit, California, AIAA 2002 - 4635, August 2002.
10. S.B. McCamish, M. Romano, X.P. Yin, "Autonomous distributed algorithm form multiple spacecraft in close proximity operations", AIAA Guidance, Navigation and Control Conference and Exhibit, Carolina USA, AIAA 2007-6857, August 2007.
11. H.B. Duan, Q.N. Luo, G.J. Ma, Y.H. Shi, "Hybrid particle swarm optimization and genetic algorithm for multi-UAVs formation reconfiguration", *IEEE Computational Intelligence Magazine*, Vol.8, No.3, pp.16-27, 2013.
12. C.H. Sun, H.B. Duan, Y.H. Shi, "Optimal satellite reconfiguration based on closed-loop brain storm optimization", *IEEE Computational Intelligence Magazine*, Vol. 8 No.4, pp 59-51, 2013.
13. J.M. Su, Y.F. Dong, "Gathering the fractionated electromagnetic satellites cluster by simulating fish school", *Aircraft Engineering and Aerospace Technology*, Vol. 84, Iss: 2, pp. 115-119, 2012.
14. J.Tian, N. Cui, R. Mu, "Optimal formation reconfiguration using genetic algorithms", *International Conference on Computer Modeling and Simulation*, China, pp.95-98, 2009.
15. A. Bilal, "Chaotic bee colony algorithms for global numerical optimization", *Expert Systems with Applications*, Vol. 37, pp.5682-5678, 2014.
16. H. Schaub, L. Junkins, *Analytical Mechanics of Space Systems* AIAA Education Series, Second Edition, Reston VA, 2003, ch 12 and 14.
17. H. Schaub, R. Srinivas, L. Junkins, T. Alfriend, "Satellite formation flying control using mean orbit elements", *Journal of the Astronautical Sciences*, Vol. 48, No. 1, pp. 69-87, 2000.
18. P. Civiolu, "Backtracking search optimization algorithm for numerical optimization problems", *Applied Mathematics and Computation*, Vol.219, pp.8121-8144, 2013.
19. J. Kennedy, R. Eberhart, "Particle swarm optimization" in *Proc IEEE International Conference on Neural Networks*, 1995, Vol. 4, pp. 1942-1948.
20. H.B. Duan, P.X. Qiao, "Pigeon-inspired optimization: a new swarm intelligence optimizer for air robot path planning", *International Journal of Intelligent Computing and Cybernetics*, Vol. 7, No. 1, 2014.